Supplementary Information

Tuning operation temperature of charging-free thermally regenerative electrochemical cycles driven by semiclathrate hydrate formation

Yohei Matsui*[1], Yuki Maeda[1]

[1]Energy Chemistry Division, Energy Transformation Research Laboratory, Central Research Institute of Electric Power Industry, Yokosuka, 240-0196, Japan

*Corresponding author

Email: y-matsui@criepi.denken.or.jp

Supplementary Figures

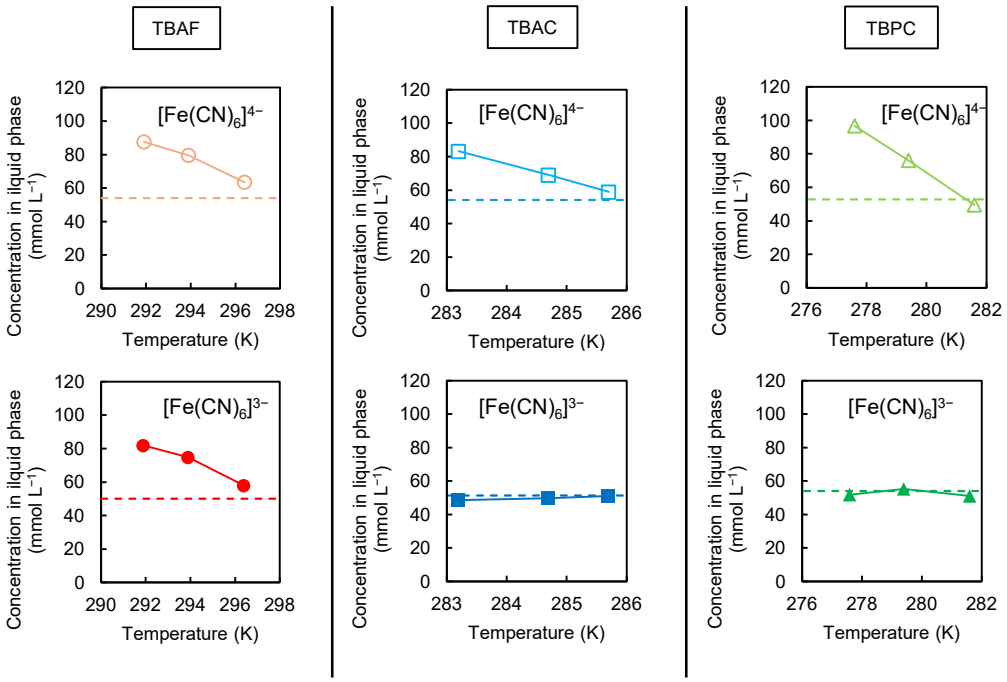

Figure S1. Concentrations of $[Fe(CN)_6]^{3-}$ and $[Fe(CN)_6]^{4-}$ in the liquid phase of TBAF, TBAC and TBPC electrolytes sampled at different temperatures. The dashed lines represent the concentrations in the state without SCH formation.
To determine the concentration, the electrolyte was maintained at a constant temperature to induce the formation of SCH and the liquid phase. The liquid phase was then collected using a syringe equipped with a filter. The collected solution was diluted using an aqueous 1 mol L^{-1} KCl solution. The concentrations of $[Fe(CN)_6]^{3-}$ and $[Fe(CN)_6]^{4-}$ in the diluted sample were quantified by chronocoulometry. A Pt disk electrode, Pt spiral electrode, and Ag/AgCl electrode were used as the working, counter and reference electrodes, respectively. As the amount of SCH increases, part of the electrolyte becomes solid, reducing the volume of the liquid phase. Therefore, if there is no association between the solute and SCH, a decrease in temperature generally increases the solute concentration in the remaining liquid phase. Consistent with this general behavior, the concentration of $[Fe(CN)_6]^{4-}$ increases upon cooling in all the electrolytes. The concentration of $[Fe(CN)_6]^{3-}$ in the TBAF electrolyte shows a similar behavior to that of $[Fe(CN)_6]^{4-}$. In contrast, in the TBAC and TBPC electrolytes, the concentration of $[Fe(CN)_6]^{3-}$ remains nearly constant even at lower temperature, indicating a selective decrease in its fraction in the liquid phase.

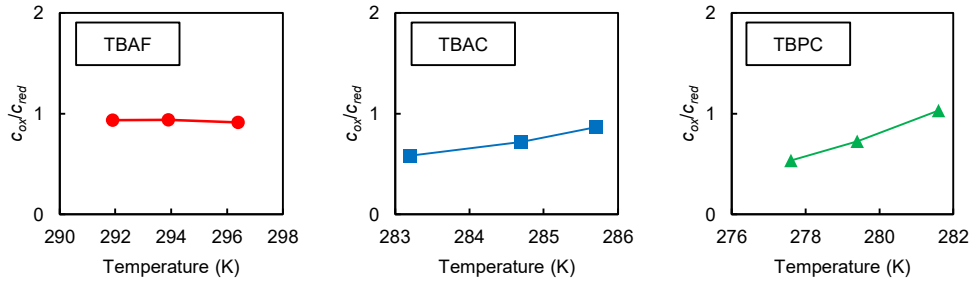

Figure S2. Effect of SCH formation on the $[Fe(CN)_6]^{3-}$ concentration ratio, which was calculated from the result of Fig. S1. c_{ox} and c_{red} represent the concentration of $[Fe(CN)_6]^{3-}$ and $[Fe(CN)_6]^{4-}$, respectively.

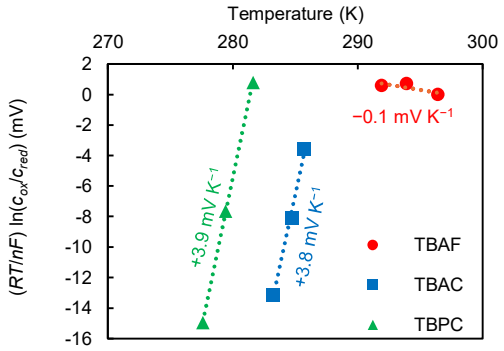

Figure S3. α_{loss} values in the TBAF, TBAC and TBPC electrolytes.

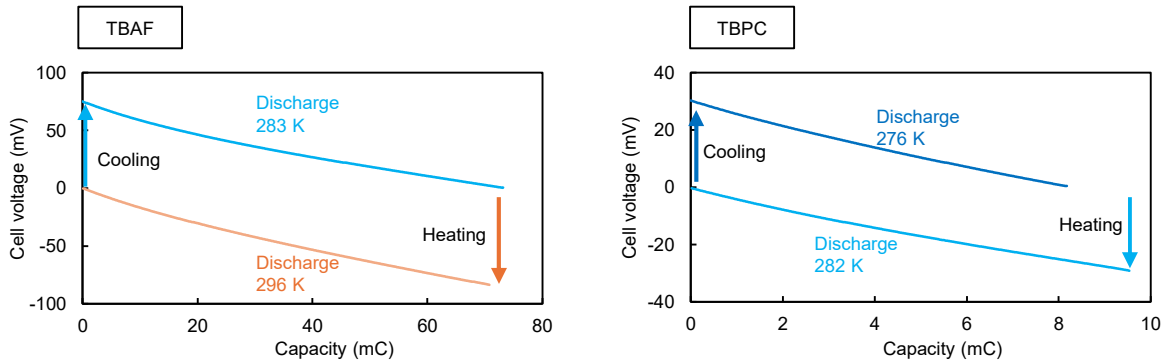

Figure S4. Second-cycle performance of the TBAF and TBPC cells.

The TBAF cell successfully operated during the second cycle, even though the applied temperature profile differed from that of the first cycle. This result confirms that the cell can work under varying thermal conditions. The TBPC cell also completed a second cycle, demonstrating the feasibility of multi-cycle operation. However, the discharge capacity in the second cycle decreased compared with the first cycle. This capacity fade suggests the presence of an underlying degradation mechanism, which will be investigated in future work.

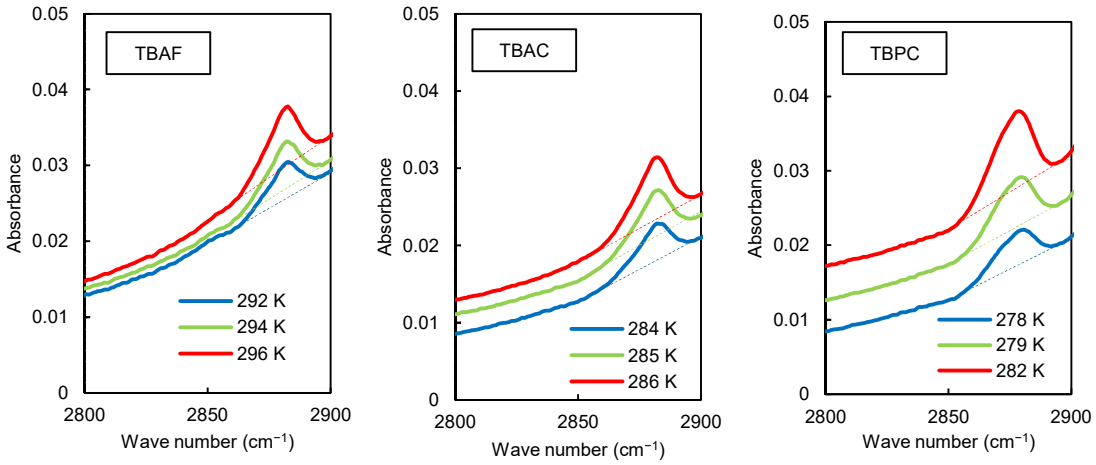

Figure S5. FT-IR spectra of the liquid phases in the TBAF-based, TBAC-based and TBPC-based electrolytes collected at different temperatures. The height of the peak derived from C−H stretching in the butyl group of the organic cations was used for the quantification of organic salt concentration in the liquid phase.

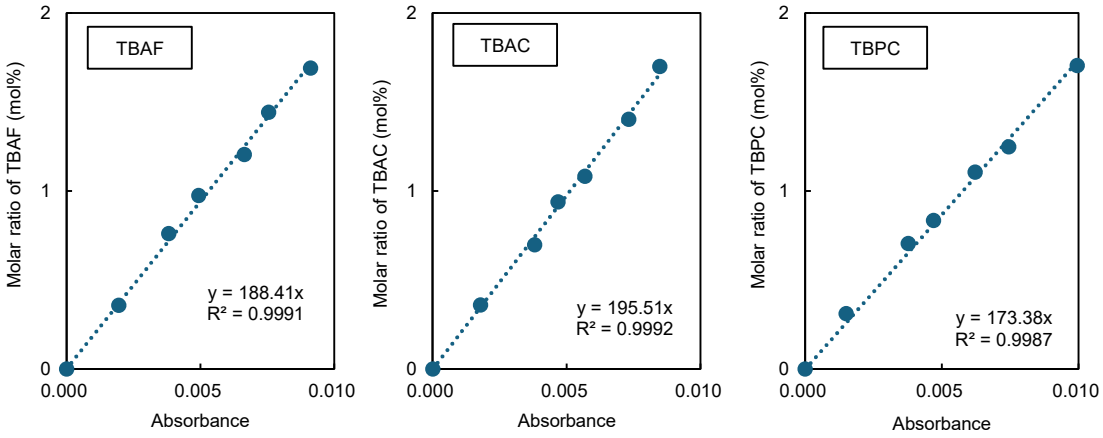

Figure S6. Qualification curves of TBAF, TBAC and TBPC based on the height of the peak derived from C–H stretching in the butyl group of the organic cations in the FT-IR spectra.